AD-A043 562   CALIFORNIA INST OF TECH PASADENA   F/G 20/4
FLAGELLA AND CILIA HYDROMECHANICS, (U)
JUL 77 T Y WU
UNCLASSIFIED   E-97B-49   N00014-76-C-0157
                                                               NL

| OF |
AD
A043562

END
DATE
FILMED
9 -77
DDC

REPORT DOCUMENTATION PAGE		READ INSTRUCTIONS BEFORE COMPLETING FORM
1. REPORT NUMBER E-97B-49	2. GOVT ACCESSION NO.	3. RECIPIENT'S CATALOG NUMBER
4. TITLE (and Subtitle) Flagella and Cilia Hydromechanics		5. TYPE OF REPORT & PERIOD COVERED
		6. PERFORMING ORG. REPORT NUMBER E-97B-49
7. AUTHOR(s) Theodore Y. Wu		8. CONTRACT OR GRANT NUMBER(s) N00014-76-C-0157
9. PERFORMING ORGANIZATION NAME AND ADDRESS California Institute of Technology		10. PROGRAM ELEMENT, PROJECT, TASK AREA & WORK UNIT NUMBERS
11. CONTROLLING OFFICE NAME AND ADDRESS Office of Naval Research The Department of the Navy Arlington, VA 22217		12. REPORT DATE July 1977
		13. NUMBER OF PAGES 22
14. MONITORING AGENCY NAME & ADDRESS(if different from Controlling Office)		15. SECURITY CLASS. (of this report)
		15a. DECLASSIFICATION/DOWNGRADING SCHEDULE

16. DISTRIBUTION STATEMENT (of this Report)

Approved for public release: Distribution unlimited

D D C
AUG 30 1977
C

17. DISTRIBUTION STATEMENT (of the abstract entered in Block 20, if different from Report)

18. SUPPLEMENTARY NOTES

19. KEY WORDS (Continue on reverse side if necessary and identify by block number)

Micro-organism locomotion
Low-Reynolds-number hydromechanics
Flagellates, Ciliates
Wall effects.

20. ABSTRACT (Continue on reverse side if necessary and identify by block number)

This talk will first make an expository survey on the recent development of the low-Reynolds-number hydrodynamics pertaining to micro organism locomotion. The scope of interest will be focused on two primary modes of swimming in this flow regime, namely the flagellar and ciliary propulsion. In order to overcome the shortcoming of classical resistive-force theory, the improved slender-body theory requires an accurate account of (1) the long-range force field generated by the flagellar motion (which is invariably of finite amplitude), (2) the interaction between the cell body and flagella, and (3) the state of self-propulsion. These basic features interrelate to make the problem interesting, the development of the refined theory challenging, and the improved accuracy being achieved for theoretical prediction doubly rewarding to both the fluiddynamicist and microbiologist for their future joint studies.

DD FORM 1473 EDITION OF 1 NOV 65 IS OBSOLETE
1 JAN 73
S/N 0102-014-6601

1977
Biomechanics
Symposium

Presented at the

1977 JOINT APPLIED MECHANICS, FLUIDS ENGINEERING,
AND BIOENGINEERING CONFERENCE

YALE UNIVERSITY
NEW HAVEN, CONNECTICUT
JUNE 15-17, 1977

Sponsored by

THE APPLIED MECHANICS DIVISION, ASME
THE BIOENGINEERING DIVISION, ASME
THE FLUIDS ENGINEERING DIVISION, ASME

Edited by

RICHARD SKALAK
COLUMBIA UNIVERSITY

ALBERT B. SCHULTZ
UNIVERSITY OF ILLINOIS
CHICAGO CIRCLE

THE AMERICAN SOCIETY OF MECHANICAL ENGINEERS

United Engineering Center   345 East 47th Street   New York, N.Y. 10017

FLAGELLA AND CILIA HYDROMECHANICS

Theodore Y. Wu

California Institute of Technology
Pasadena, California 91125

Abstract

This talk will first make an expository survey on the recent development of the low-Reynolds-number hydrodynamics pertaining to micro-organism locomotion. The scope of interest will be focused on two primary modes of swimming in this flow regime, namely the flagellar and ciliary propulsion. In order to overcome the shortcoming of classical resistive-force theory, the improved slender-body theory requires an accurate account of (1) the long-range force field generated by the flagellar motion (which is invariably of finite amplitude), (2) the interaction between the cell body and flagella, and (3) the state of self-propulsion. These basic features interrelate to make the problem interesting, the development of the refined theory challenging, and the improved accuracy being achieved for theoretical prediction doubly rewarding to both the fluiddynamicist and microbiologist for their future joint studies.

INTRODUCTION

In nature the phenomena of locomotion of aquatic animals in aqueous media embraces a great variety of species with different sizes, different modes of swimming motion, and with varying biophysical basis of physiology and metabolism. Of these families of swimming organisms, the size spans over an impressive nineteen orders in magnitude; their basic mechanism of swimming ranges from the viscosity-dominant, inertialess fluid reactions for micro-organisms in one extreme to the inertia-based reactive hydro-mechanics for larger animals in the other. In physiology, the metabolic processes vary from the better known conversion of chemical energy to mechanical work by means of muscular contractile effort in higher animals to the not-so-fully understood processes in prokaryotic flagella of bacteria in which no enzymatic activities are known to exist. Evidently this subject is interdisciplinary in nature, and its development would be most rewarding if cultivated by a joint team of biologists and fluid-dynamicists.

The world of micro-organisms that can perform swimming motion may be classified, according to their modes of movement, into three major categories.

1. **Flagellates.** Flagellates, such as the various kinds of spermatozoa and many flagellated bacteria, locomote themselves by means of undulatory movement of a single flagellum or several bundles of flagella, in the formation of planar waves (e. g. Ceratium, Ochromonas, Prymnesium), helical waves (e. g. Trichomonas, Trachelomonas), or of three-dimensional waves of a more general type (e. g. In Euglena and Peranema). Further variations of these basic forms include the spirilla, spirochaetes, and the flagellar-mastigoneme propulsion system.

2. **Ciliates.** The ciliates are a class of protozoa which have a large number of hair-like organelles, called cilia, attached to the cell surface in a fairly regular row-and-column distribution, performing a beat pattern inherent to each species to form a metachronal wave in propulsion. Some of the common ciliates, whose motion has been more extensively studied, include Paramecium, Tetrahymena, Spirostomum, and Opalina. The ciliary mode of propulsion is found not only in ciliates, but also in some organs of higher animals such as the muco-ciliary systems in respiratory trachea and in reproductive ducts. It is in the latter problem areas that further development of ciliary dynamics and physiology will have a most active future.

3. **Pseudopods.** The temporary protrusion and retractile process of the protoplasm of a cell for moving about, such as in amoebic movement involves certain mechanism of intracellular flow and cytoplasmic streaming. This mode of movement appears to be the least understood of the three, and, for this reason, the present discussion will be devoted to the first two types of propulsive movements.

From the hydromechanical point of view, these movements have three important features which are essential to our basic understanding. (I) First, the motion is generally characterized by two small Reynolds numbers, one based on the mean propulsion velocity and the other on the oscillatory component of the motion; they may be expressed as

$$Re_U = Ul/\nu , \qquad Re_\omega = \omega b^2/\nu , \qquad (1)$$

where U denotes the mean propulsion velocity of a micro-organism of length l, ω the radian frequency of an undulating flagellum or cilium of cross-sectional radius b, and ν is the kinematic viscosity coefficient of an aqueous medium ($\nu = 0.01$ cm2/sec.). Typically, Re_U ranges from 10^{-6} for small bacteria to 10^{-2} for most spermatozoa, and Re_ω is approximately an order of magnitude smaller. At such low Reynolds numbers, the fluid motions so produced are dominated by the viscous force while the inertial effects, of both the fluid and the microscopic body, are entirely negligible. This means that the flow would altogether stop as soon as the propulsive motion is halted. (II) Further, the velocity field generated by the motion of a body element has the longest range known in fluid mechanics and the motion is invariably of a finite amplitude. These features combine to make the hydromechanical analysis both interesting and challenging. The ratio of the amplitude, h, of a flagellar or ciliary wave to the wavelength, λ, is typically about 1/7. The recent efforts have been directed primarily to improve the theory so that the effect of flagellar curvature can be more accurately determined for motions of such large amplitude. (III) In a broad sense, move-ment of prokaryotic flagellates and of eukaryotic ciliates and flagellates can be regarded as self-propelled, i. e. without aid of any extraneous force and moment of force. The mathematical expression of the state of self-propulsion is, symbolically,

$$\Sigma \text{ forces} = 0 , \qquad \text{and} \qquad \Sigma \text{ moments} = 0 , \qquad (2)$$

where the sign Σ includes the summation by the limiting process of integration. This means that while we need to use forcelets and their moments to represent the propulsive action of flagella and cilia, the resultant force and moment must always vanish, even when the micro-organism accelerates along a rectilinear or curvilinear path, because the inertia of both the fluid and the body is negligible. This implies that the fluid at some distance away from a self-propelling body will already feel no trace of a net force and moment; it may sense at most certain higher moments of a force distribu-tion. As a result, this feature brings forth some unique flow behaviors that are by their very nature absent in low-Reynolds-number hydromechanics of inanimated small objects. In combination, the above basic features of flow pertaining to micro-organism locomotion will form an overall basis for the present discussion.

The rapid development of the general subject on micro-organism locomotion can be attributed to the stimulation provided by the pioneering work of Sir James Gray (1928, 1968) and Sir Geoffrey Taylor (1951, 1952a, b). Recent advances in this active field have been reported extensively in the literature, especially in the volumes by Sleigh (1973), Lighthill (1975a), Wu, Brokaw & Brennen (1975), and in the review articles by Jahn & Votta (1972), and Brennen & Winet (1976).

FUNDAMENTAL FLOW SINGULARITIES

In order to help us appreciate the recent development, in both its bio-physical and mathematical contents, of this general subject, it is useful to have an introductory disclosure of the basic tools which have been employed by the applied mathematician and hydrodynamicist for this class of problems.

Insofar as the inertial effects are negligible, the hydrodynamics of low-Reynolds-number flows can be prescribed by the Stokes equations

$$\nabla \cdot \underline{u} = 0 , \tag{3}$$

$$\nabla p = \mu \nabla^2 \underline{u} + \underline{f}(\underline{x}, t) . \tag{4}$$

where $\underline{u}$ denotes the flow velocity, p the pressure, μ the dynamic viscosity coefficient ($\mu = \rho\nu$, ρ being the fluid density), and $\underline{f}$ represents a generalized distribution of extraneous force which may depend on the radius vector $\underline{x}$ and time t. The primary fundamental solution of the linear system (3) and (4) corresponding to $\underline{f}$ being a singular point force in an unbounded fluid was discussed by Oseen (1927), Burgers (1938), and called a Stokeslet by Hancock (1953). The higher-order poles associated with a Stokeslet have been explored by Batchelor (1970) Blake (1971-74), Chwang and Wu (1971-76) and others. A brief description of the properties of these flow singularities can be given as follows.

(i) Stokeslet. — A Stokeslet of strength $\underline{\alpha}(t)$ corresponds to having

$$\underline{f} = 8\pi\mu\underline{\alpha}(t) \, \delta(\underline{x}) , \tag{5}$$

where $\delta(\underline{x})$ denotes the Dirac delta function. Its induced velocity and pressure fields are, respectively,

$$\underline{U}_S(\underline{x};\underline{\alpha}) = \underline{\alpha}/r + (\underline{\alpha} \cdot \underline{x}) \underline{x}/r^3 , \tag{6}$$

$$P_S(\underline{x};\underline{\alpha}) = -2\mu \nabla \cdot (\underline{\alpha}/r) , \qquad (r = |\underline{x}|). \tag{7}$$

It exerts on the fluid a net force

$$\underline{F}_S = 8\pi\mu\underline{\alpha}(t) , \tag{8}$$

which requires an equal and opposite force acting on the fluid at infinity in order to maintain dynamic equilibrium. The velocity is seen to fall off like r^{-1}, a rate which is not surpassed by any other known flow singularities. The evidence of this long-range effect can be detected from the resulting streamlines (see Fig. 1), showing that fluid is drawn in from behind to approach the singular force and is then thrust forward along divergent paths with a fore-aft symmetry.

(ii) Rotlet. — A rotlet of strength $\underline{\gamma}(t)$ is associated with the singular moment of force

$$\underline{f} = 4\pi\mu \nabla \times \underline{\gamma}(t) \, \delta(\underline{x}) , \tag{9}$$

the resulting flow velocity and pressure being

Fig. 1. The streamlines due to a Stokeslet of strength $\underline{\alpha}$, shown in a meridian plane about the axis of symmetry.
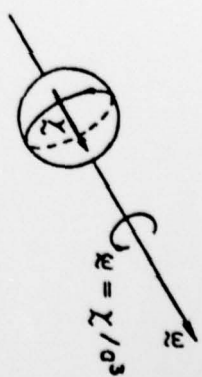

Fig. 2. The flow field due to a rotlet of strength $\underline{\chi}$, visualized as the one due to a rotating sphere of small radius a with angular velocity $\underline{\omega}$.

$$\underline{U}_R(\underline{x}, \underline{\gamma}) = \nabla \times (\underline{\gamma}/r) , \qquad P_R = 0 . \tag{10}$$

It exerts on the fluid a net moment

$$\underline{M}_R = 8\pi\mu\underline{\gamma}(t) , \tag{11}$$

which is balanced by an equal and opposite moment on the fluid at infinity. Physically, the flow field of a rotlet may be visualized as the one due to a small sphere of radius a rotating about the $\underline{\gamma}$-axis with angular velocity the $\underline{\gamma}$-axis, with flow speed falling off like r^{-2}.

(iii) Stresslet. — A stresslet is a component of the Stokes force-dipole defined by

$$\underline{U}_{SD}(\underline{x};\underline{\alpha},\underline{\beta}) = -\underline{\beta} \cdot \nabla \underline{U}_S(\underline{x};\underline{\alpha}) = \underline{U}_R + \underline{U}_{SS} , \tag{12}$$

where $\underline{U}_R$ represents a rotlet of strength $\underline{\gamma} = \underline{\beta} \times \underline{\alpha}$, and

$$\underline{U}_{SS}(\underline{x};\underline{\alpha},\underline{\beta}) = -(\underline{\alpha} \cdot \underline{\beta})\underline{x}/r^3 + 3(\underline{\alpha} \cdot \underline{x})(\underline{\beta} \cdot \underline{x}) \underline{x}/r^5 , \tag{13}$$

is the stresslet velocity field. This velocity is symmetric with respect to interchange of $\underline{\alpha}$ and $\underline{\beta}$, and represents a pure straining or extensional flow (see Fig. 3). Like the rotlet, the stresslet has its velocity decreasing like r^{-2} as $r \to \infty$.

(iv) Mass doublet. — A mass doublet, of strength $\underline{\beta}$, has the same velocity field as that of a dipole known in potential flow; it is also the Laplacian of a Stokeslet:

$$\underline{U}_D(\underline{x};\underline{\beta}) = \nabla\nabla \cdot (\underline{\beta}/r) = -\frac{1}{2} \nabla^2 \underline{U}_S(\underline{x};\underline{\beta}) . \tag{14}$$
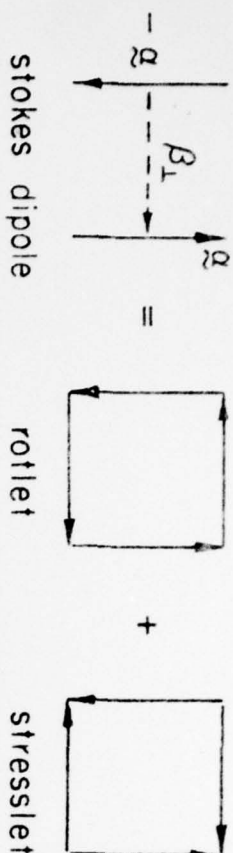
Fig. 3. Decomposition of a Stokes dipole into a rotlet and a stresslet.

It has zero vorticity since $\underline{\nabla}D$ possesses a scalar potential and it carries no pressure on account of the negligible inertia effects.

Higher-order flow singularities can be readily derived from the above fundamental cases; they are useful in construction of exact solutions (Chwang & Wu 1975) and especially when a high degree of accuracy is required (Chwang 1975).

RESISTIVE-FORCE THEORY

In the general case of flagellar movement, approximate calculation of the highly viscous flow past a slender body, such as a flagellum, can be carried out by applying resistive-force theory which seeks a definite relationship between the force exerted by the body per unit length on the fluid and the local velocity of the flagella. The central concept of the theory is quite simple. Suppose a segment of a slender flagellum of arc length ds moves with velocity $\underline{V}(s,t)$ (relative to the unperturbed fluid far away) so that its component tangential to the body centreline is V_s and the complementary normal component is V_n. The resistive force exerted by the segment on fluid has two components dF_s and dF_n in the same two directions which can be expressed as

$$dF_s = C_s \mu V_s \, ds , \qquad dF_n = C_n \mu V_n \, ds , \qquad (15)$$

where C_s and C_n are two dimensionless force coefficients assumed to be dependent only on the instantaneous body geometry and independent of the segment position s or its velocity. For an elongated body of nearly circular cross section, the force coefficients assume for a quite general category of motion the expression

$$C_s = \frac{2\pi}{\log(2q/b) - C_1} , \qquad C_n = \frac{4\pi}{\log(2q/b) + C_2} , \qquad (16)$$

where b is the local or a characteristic cross-sectional radius of the flagellum and q denotes a length whose value depends, together with the two numerical constants C_1 and C_2, on body geometry as well as the type of flagellar movement. For instance, for an elongated prolate spheroid with semi-axes a and b $(b \ll a)$ (16) is accurate with a relative error of $O(b/a)^2$ (Tillett 1970) if

$$q = a , \qquad C_1 = C_2 = \frac{1}{2} . \qquad (17)$$

The local force coefficients of a flagellum in undulatory movement are much more difficult to determine accurately. It was Hancock (1953) who first applied a line distribution of Stokeslet and mass doublet to represent a slender body movement, and, based on a limiting result of his analysis, Hancock proposed the form (16) with

$$q = l/2 , \qquad C_1 = C_2 = \frac{1}{2} \quad \text{(Hancock 1953)} \qquad (18)$$

where l is the length of the filament. Subsequently, Gray & Hancock (1955) introduced for computing flagellar motions the formula (16) with

$$q = \lambda , \quad C_2 = \frac{1}{2} , \quad C_1 = C_2 = \frac{1}{2} C_n \quad \text{(Gray-Hancock)} \qquad (19)$$

where λ is the wavelength of a planar or helical flagellar wave. The popularity of this formula is evidently related to the simplicity of the resulting mathematical analysis. The theory, however, is crude and its accuracy is insufficient for making more refined studies by our modern standard. Along this line of development Lighthill (1975b) has recently re-examined the hydrodynamics of flagellar locomotion and suggested that for flagellar waves it is accurate to take

$$q = 0.09 \lambda , \quad C_1 = 0 , \quad C_2 = \frac{1}{2} \quad \text{(Lighthill 1975b).} \qquad (20)$$

To provide an order estimate of the accuracy of these formulas, we recall the theory for straight slender bodies (of length l) developed by Tuck (1964), Tillett (1970), Batchelor (1970), and Cox (1970). Based on expansion of the line-force distribution in terms of a series in inverse powers of $\log (l/b)$, the theory shows that q actually depends on s for arbitrary body shape except for slender spheroids. But as an approximation, formula (16) with constant values of q, C_1, C_2 can still be used (e.g. $q = l/2$, $C_1 = +0.807$, $C_2 = 1 - C_1$ for a circular cylinder) if we accept that the error is of order $[\log^2 (l/b)]^{-\frac{1}{2}}$. With such errors, the accuracy of the crude resistance coefficients is generally regarded as insufficient for the scientific requirements and becomes even more questionable when the body centreline bends and waves as in flagellar motions.

The need of having an improved slender-body theory was stressed and extensively discussed, among other basic problems, during the Pasadena Symposium on Swimming and Flying in Nature (Proceedings edited by Wu, Brokaw & Brennen 1975). This problem was further pursued at the Cambridge Symposium on Biodynamics of Animal Locomotion which was organized by Professor Sir James Lighthill and Professor Torkel Weis-Fogh (Proceedings edited by Lighthill & Pedley, to be published by Academic Press). From these rounds of discussion we may single out the following observations.

Based on a series of experiments using mechanical models, Chwang and Wu (1975b) found considerable discrepancies between theory and experiment. Of the significant factors that may contribute to these discrepancies, we have subsequently identified: (i) the effect of finite curvature of body centreline, (ii) the wall effects due to the proximity of the container boundary (both in model and prototype tests), and (iii) the inertia effect that may arise when the Reynolds number based on the mechanical model length is no longer small (even when the body centreline is moving perpendicular to itself).

New research has been pursued along these identified directions. The first test case is the slender circular ring (the only shape with a uniformly curved centreline yet without body ends). For the Stokes flow involving a ring in arbitrary motion we have found that the solution can be determined asymptotically to any specified order of accuracy, at least in principle, by including higher-order flow singularities. This ring solution has been instructive in guiding us to establish a refined slender-body theory for the

general case of arbitrary body motion with finite amplitude. Development of flagella and cilia hydromechanics, again no exception like many major fields of fluid mechanics, has been full of challenge, perplexity and excitement.

Before I proceed with my report on this task, we conclude this section by noting that the force calculation must be complemented by the considera- tion of a pure couple (See Chwang & Wu 1971) acting on the fluid by a segment of flagellum whose surface undergoes a spin with angular velocity Ω_s paral- lel to the unit vector $\hat{S}_s$ directed along the body centerline. The corres- ponding moment is

$$d\underset{\sim}{M}_s = C_M \mu b^2 \underset{\sim}{\Omega}_s ds , \qquad C_M = 4\pi . \qquad (21)$$

Unlike the force coefficients, this formula remains accurate as the body length is increased, whatever the value of the Reynolds number based on Ω_s and body length ℓ may be (Chwang & Wu 1974).

THE STOKES FLOW PAST A SLENDER RING

In order to investigate the body-centerline curvature effect in Stokes flow, Wu & Johnson (1976) have selected a slender ring as the primary test case. It is of interest to summarize here the new result and to ascertain, by comparison, the deficiencies of the previous theories in predicting sectional forces, and moments. The mathematical details, however, will be curtailed since they are beyond the present scope.

The result is presented below separately for four basic modes of motion, namely (i) broadwise translation, (ii) edge-on translation (in centerline plane), (iii) rotation about the central axis, and (iv) on-edge rotation. The general case of arbitrary motion can be resolved by superposition of these solutions.

(i) Broadwise rotation — Consider a slender ring characterized by a small parameter $\epsilon = b/a \ll 1$, where a,b are its major and minor axes, respec- tively (a being the radius of the centerline circle and b the cross-sectional radius). When the ring moves with velocity V parallel to its central axis (z-axis say), the following flow singularities, distributed uniformly along the centerline, are required to represent the flow, with their line densities:

Stokeslet	(along $\hat{e}_z$)	$\alpha = \frac{1}{2}V/(L + \frac{1}{2})$,
doublet	($-\hat{e}_z$)	$\beta = \frac{1}{2}b^2\alpha$,
rotlet	($-\hat{e}_\theta$)	$\gamma = \frac{1}{4}Vb\epsilon(L-1)/(L+\frac{1}{2})$
stresslet	($\hat{e}_r, \hat{e}_z$)	$A = \frac{1}{2}b\alpha$,
quadrupole	($\hat{e}_r, \hat{e}_z$)	$B = -\frac{1}{4}b^2A$.

(22)

Here, $(\hat{e}_r, \hat{e}_\theta, \hat{e}_z)$ denote the base vectors in the cylindrical polar coordi- nates (r, θ, z), and L stands for

$$L = \log(8/\epsilon) , \qquad \epsilon = b/a \ll 1 . \qquad (23)$$

We note that the Stokeslet and doublet are required for the solution of flow velocity $\underset{\sim}{u}$ up to $O(L^{-n})$ for any positive integer n, and inclusion of the next three singularities reduces the error of solution for $\underset{\sim}{u}$ to $O(\epsilon^2 \log \epsilon)$, which is a considerable refinement.

(ii) Edge-on translation — When the ring moves in the x-direction (taken to be $\theta = 0$) with velocity

$$\underset{\sim}{V} = \hat{e}_r V_n - \hat{e}_\theta V_s , \qquad V_n = V\cos\theta , \qquad V_s = V\sin\theta , \qquad (24)$$

the required centerline distributions of leading singularities are found to be

Stokeslet	($\hat{e}_r$)	$\alpha_n = \frac{1}{2}V_n(L-3)/(L^2 - \frac{5}{2}L-1)$,
	($-\hat{e}_\theta$)	$\alpha_s = \frac{1}{4}V_s b(L-\frac{5}{2})/(L^2 - \frac{5}{2}L-1)$,
doublet		$\beta = -\frac{1}{2}b^2 \alpha$.
rotlet	($\hat{e}_z$)	$\gamma = \frac{3}{4}V_s b\cdot(L^2 - \frac{29}{6} L+\frac{11}{2})/(L^2 - \frac{5}{2}L-1)$,
stresslet	($\hat{e}_r, \hat{e}_r$)	$A = \frac{3}{4}V_n b(L - \frac{17}{6})/(L^2 - \frac{5}{2}L-1)$,
quadrupole	($\hat{e}_r, \hat{e}_r$)	$B = -\frac{1}{4}b^2A$.

(25)

The velocity field $\underset{\sim}{u}$ represented by these flow singularities is accurate up t) a small error term of $O(\epsilon^2 \log \epsilon)$. However, it is of significance to note that in this case, the resulting force coefficients, $C_n = 8\pi a_n/V$, no longer assume the classical form (16); this departure is evidently due to the effect of the centerline curvature.

(iii) Rotation about the central axis — For the case when the ring rotates about the z-axis with angular velocity Ω, we have a uniform centerline distribution of Stokeslet and rotlet, with strengths

Stokeslet	($\hat{e}_\theta$)	$\alpha = \frac{1}{4}\Omega a/(L-2)$,
rotlet	($\hat{e}_z$)	$\gamma = 3b\alpha(L - \frac{7}{3})$.

(26)

In this case the error of $\underset{\sim}{u}$ is also of $O(\epsilon^2 \log \epsilon)$.

(iv) Edge-on rotation — In this mode the ring rotates about the x-axis with angular velocity Ω so that at the instant when the centerline coincides with the $y = 0$ plane the velocity of the centerline is

$$\underset{\sim}{V} = V_n\hat{e}_z , \qquad V_n = \Omega a \sin\theta .$$

The corresponding flow singularities have the following line densities:

Stokeslet	($\hat{e}_z$)	$\alpha = \frac{1}{2}V_n a/(L - \frac{3}{2})$,
doublet	($-\hat{e}_z$)	$\beta = \frac{1}{2}b^2\alpha$,
rotlet		$\gamma = b\alpha[\hat{e}_r \cot\theta - \frac{3}{2}(L - 2)\hat{e}_\theta]$,
stresslet	($\hat{e}_r, \hat{e}_z$)	$A = \frac{1}{2}b\alpha$,
quadrupole	($\hat{e}_r, \hat{e}_z$)	$B = -\frac{1}{4}b^2A$.

(27)

(28)

The above results show that the sectional force coefficients have various forms depending on the curvature and modes of motion. In applications to flagellar motion, $\log(\ell/b)$ usually ranges from 3 to 5 (corresponding to
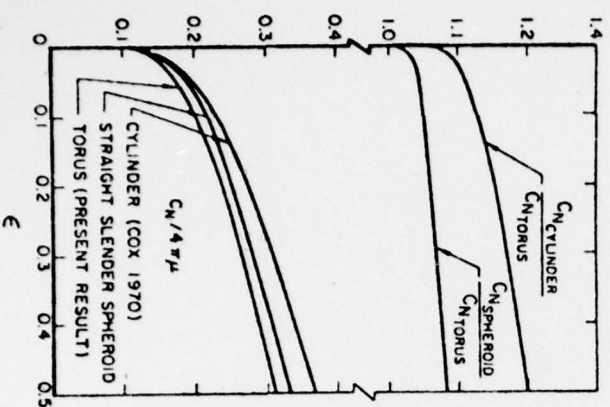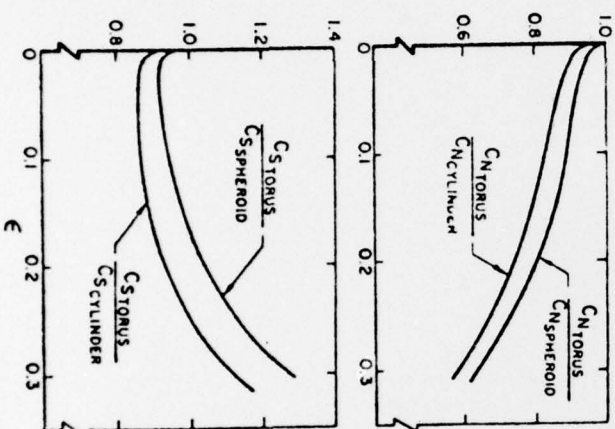
Fig. 4. Broadwise motion of torus.

Fig. 5. Comparison for torus translating in its own plane.
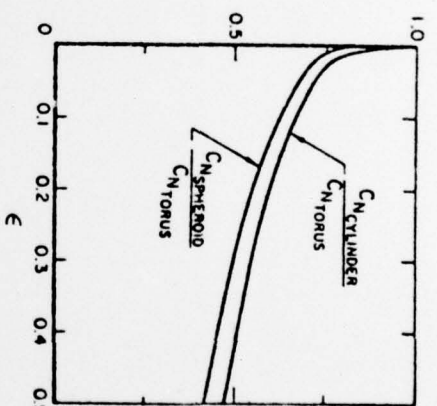
Fig. 6. Torus rotating in its plane.

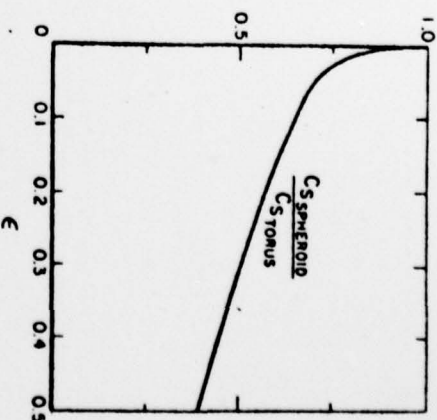Fig. 7. On-edge rotation of torus.

ℓ/b = 20 to 150). For such moderate values of L, expansion of the rational functions of L in the above expressions into series of L^{-1} may induce unnecessary error. In this sense the present result can provide a useful guideline for developing the general slender-body theory to be discussed below. Further, we note that the rollet γ will yield a pure couple; this contribution may be significant, especially when the net moment of Stokeslet force is small. The presence of rollet may even cast new light on the mechanism of spirochete locomotion as discussed by Chwang, Winet & Wu (1974).

To exhibit the difference between the new results and classical resistive-force theory, we present the numerical results in Figures 4-7 for the four basic modes of torus motion. The comparison shows that while the difference is not large for the translational modes (less than about 15% for $\epsilon < 0.1$), it is quite significant in the two cases of rotation. This may be attributed to the feature that in rotation the body velocity has finite variations, both in magnitude and in direction, along the torus. On physical ground we may expect that changes in phase along a flagellum or cilium in undulatory motion would have a similar effect on the force coefficients.

GENERAL SLENDER-BODY THEORY

Johnson (1976) has considered the general case of a slender body with circular cross-section $b(s)$ of arbitrary distribution but with spheroidal-shaped ends,

$$b = \epsilon(\ell^2 - s^2)^{1/2} \quad \text{for } (1-s^2/\ell^2) \ll 1, \quad \epsilon = b_0/\ell \ll 1, \quad (29)$$

where s is the arc length along the body centerline:

$$\underline{x} = \underline{x}_0(s,t) \quad (-\ell \leqslant s \leqslant \ell), \quad (30)$$

the movement of $\underline{x}_0$ being assumed arbitrary. At each point $\underline{x}_0$ on the centerline we attach a set of orthogonal base vectors $(\underline{e}_s, \underline{e}_n, \underline{e}_b)$, pointing in the tangential, normal, and binormal directions, respectively. (see Fig. 8) i.e.

$$\underline{e}_s = \partial\underline{x}_0/\partial s, \quad \underline{e}_n = a\partial\underline{e}_s/\partial s, \quad \underline{e}_b = \underline{e}_s \times \underline{e}_n,$$

where $a(s,t)$ is the centerline radius of curvature, $a = |\partial\underline{e}_s/\partial s|^{-1}$ (31)

The velocity of material points on the body surface is due to the translation of centerline with velocity $\partial\underline{x}_0/\partial t$, a surface spin about centerline with angular velocity $\Omega(s,t)\underline{e}_s$, Ω being arbitrary, and the rotation of centerline with angular velocity $\underline{\Omega}_r^s = \underline{e}_s \times (\partial\underline{e}_s/\partial t)$. Thus the no-slip boundary condition on the body surface is given by

$$\underline{u} = \dot{\underline{x}}_0 + b(s)[\Omega_s \underline{e}_s + \underline{e}_s \times \dot{\underline{e}}_s] \times \underline{e}_{r_1}$$

$$= V_s \underline{e}_s + V_n \underline{e}_n + V_b \underline{e}_b, \quad (32)$$
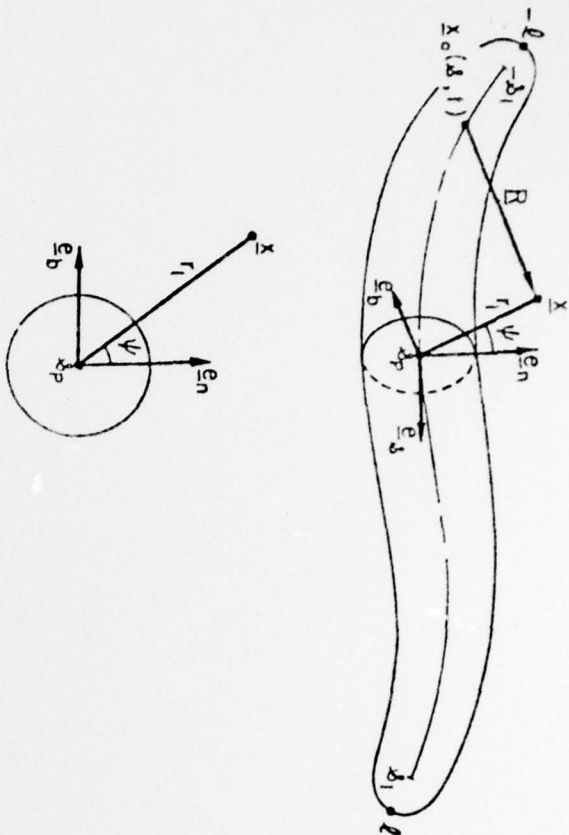
Fig. 8. The geometry and coordinates adopted for a slender-body in arbitrary movement.

where the dot denotes differentiation with respect to t, and

$$\dot{\underline{e}}_{r_1} = \hat{\underline{e}}_n \cos \psi + \hat{\underline{e}}_b \sin \psi . \tag{33}$$

The solution of the resulting Stokes flow can be represented by the distribution of necessary fundamental singularities on the body centerline as follows:

$$\underline{u}(\underline{x},t) = \int_{-s_o}^{s_o} \{ \underline{U}_S(\underline{R};\underline{q}) + \underline{U}_D(\underline{R};\underline{\beta}) + \underline{U}_R(\underline{R};\underline{\gamma}) + \underline{U}_m(\underline{R};m) + A_1\underline{U}_{SS}(\underline{R};\hat{\underline{e}}_n,\hat{\underline{e}}_n)$$
$$- B_1\underline{U}_Q(\underline{R};\hat{\underline{e}}_n,\hat{\underline{e}}_n) + A_2\underline{U}_{SS}(\underline{R};\hat{\underline{e}}_n,\hat{\underline{e}}_b) - B_2\underline{U}_Q(\underline{R};\hat{\underline{e}}_n,\hat{\underline{e}}_b) \} \, ds , \tag{34}$$

where

$$\underline{R} = \underline{x} - \underline{x}_o(s) , \qquad R = |\underline{R}| , \tag{35}$$

$$s_o = (l^2 - b^2)^{1/2} \sim (1 - \tfrac{1}{2}\epsilon^2) l . \tag{36}$$

$\underline{U}_S, \underline{U}_D, \underline{U}_R, \underline{U}_{SS}$ have been given before, $\underline{U}_D(\underline{R};m) = m\underline{R}/R^3$ is the contribution of a mass source of strength m, and $\underline{U}_Q(\underline{R};\delta,q) = (\delta \cdot \nabla)\underline{U}_D(\underline{R};q)$ denotes a quadrupole. The limits of integration $\pm s_o$ are given by the generalized foci.

The integrand in (34) is expanded in the neighborhood of the body (i.e. for $r_1 \ll l$) at each station s. Upon integration and then applying the boundary condition (32), neglecting the terms of $O(a\epsilon \log \epsilon)$, we obtain the following integral equation for $\underline{g}$.

$$\underline{V}_v(s,t) = a_v(s,t)\underline{L}_v + \int_{-s_o}^{s_o} K_v(\underline{R}_o;\underline{q})ds' , \qquad (v = s,n,b) . \tag{37}$$

where

$$L_s = 2[2 \log(2/\epsilon_*) - 1] , \qquad L_n = L_b = 2 \log(2/\epsilon_*) + 1 ,$$

$$K_v(\underline{R}_o;\underline{q}) = \frac{a_v(s',t)}{R_o} + \frac{(\underline{q}(s',t)\cdot\underline{R}_o)R_o|R}{R_o^3} - \frac{D_v a_v(s,t)}{|s-s'|} , \tag{38}$$

$$\underline{R}_o = \underline{x}_o(s,t) - \underline{x}_o(s',t) = R_{os}\hat{\underline{e}}_s + R_{on}\hat{\underline{e}}_n + R_{ob}\hat{\underline{e}}_b .$$

$$D_s = 2, \quad D_n = D_b = 1 , \quad \epsilon_* = b(s)/l(1-s^2)^{1/2} ,$$

$$\underline{g}(s,t) = a_s\hat{\underline{e}}_s + a_n\hat{\underline{e}}_n + a_b\hat{\underline{e}}_b . \tag{39}$$

Here, the base vectors $\hat{\underline{e}}_s, \hat{\underline{e}}_n, \hat{\underline{e}}_b$ in the expression (37) assume their value at s where $\underline{V}_v(s,t)$ is specified. The integral equation (37) can be solved by applying certain appropriate iteration schemes or the method of collocation. These numerical methods have been applied to evaluate the sectional force coefficients of a flagellum performing a planar or a helical wave motion. A similar theory has been introduced by Keller & Rubinow (1976) for the leading singularities, namely the Stokeslet and doublet, but with their line densities only approximately determined near the body ends.

WALL EFFECTS

Low-Reynolds-number flow theory has applications in several fields of growing importance, for instance in biophysical and biomedical applications, rheology, suspension mechanics, aerosol physics, and micro-organism motions. In these applications it is often necessary to analyze the motion of slender bodies such as fibers or organisms in the vicinity of solid boundaries since their motion is considerably modified due to the wall effects. Of these phenomena some appear in natural scheme of life (e.g. the muco-ciliary propulsion system in trachea and spermatozoa transport in ciliated duct), some are results of artificial design (e.g. the flow of suspensions during engineering processing), while many others are caused by necessary preparation for microscopic observation. We thus see the importance of wall effects in low-Reynolds-number flow, both from the standpoint of basic understanding and data interpretation. The general problem, however, is difficult, and as a result, only a few relatively simple cases have been considered.

The image system for a Stokeslet and higher-order poles into a plane wall can be derived from the classical work of Lorentz (1907), as illustrated by Burgers (1938), and more systematically identified by Blake (1971a, b, 1974), Blake & Chwang (1974). This method has been applied by Brenner (1962) to discuss arbitrary bodies, and by DeMestre (1973) for the case of circular cylinders near a plane wall, and by DeMestre & Russel (1975) to study rotating rod motions. Further applications have been made by Winet (1973), Blake & Sleigh (1974), Katz (1974), Katz & Blake (1975), Katz, Blake & Paveri-Fontana (1975), and by Aderogba (1976) for various studies of ciliary and micro-organism propulsion. A review of these contributions can be found in Brennen & Winet (1976). As an overall summary of these results,

the following feature is noteworthy from both the hydromechanical and the energetics points of view.

Generally speaking, the drag increase in drag of a slender body is always smaller in axial motion than that when the motion is transverse to the longitudinal body axis, whatever its inclination with respect to the nearby wall, i.e.

$$C_s = C_{so}(1 + \delta_s) , \quad C_n = C_{no}(1 + \delta_n) , \quad 0 < \delta_s < \delta_n ,$$
(40)

where C_{so} and C_{no} are the axial and normal force coefficients of a given body in unbounded flow, (i.e. for vanishing ratio of the body length to the distance from a wall, $l/h = 0$), and the relative increments δ_s and δ_n depend on $\lambda = l/h$ and on the body orientation with respect to the wall. The ratio of C_s to C_n is, by (40),

$$\gamma = C_s/C_n = (C_{so}/C_{no})(1 + \delta_s)/(1 + \delta_n) < C_{so}/C_{no} = \gamma_o .$$
(41)

Thus, the force-coefficient ratio γ is generally reduced by the wall effect, and this is a result of especial significance. As pointed out by Lighthill (1969), the force-coefficient ratio γ plays an important role in swimming propulsion. It relates to the maximum forward velocity, V_{max}, and to the maximum efficiency of locomotion, η_{max}, of a flagellum according to

$$V_{max}/c_b = \frac{1}{2}(1 - \gamma),$$

$$\eta_{max} = (1 - \sqrt{\gamma})^2 ,$$
(42)

where c_b is the phase velocity of flagellar wave with respect to body, and η_{max} is reached at $V/c_b = 1 - \sqrt{\gamma}$. In unbounded flow, $\gamma = 1/2$ is the lower limit reached only by extremely slender spheroids, and, as pointed out by Wu (1975), no swimming in the microscopic world would be feasible if γ could attain the value $\gamma = 1$. In most cases of micro-organism locomotion, γ ranges between 0.6 and 0.7. In this rather narrow range of γ in practical operation, we thus see (from (41) and (42)) the possible advantage for a slender body to swim near a wall since the value of γ can thereby be somewhat decreased (by about 10 - 15%), giving both higher swimming velocity and propulsive efficiency.

The general problem of wall effect can be formulated for the case of a plane wall by incorporating the known image systems. Suppose that the velocity of an unbounded Stokes flow due to a slender body with given movement is known, which can always be expressed as

$$\underset{\sim}{u}_o = \int_{-s_o}^{s_o} \{\underset{\sim}{z}\phi(\underset{\sim}{x};s,t) - \nabla[(\underset{\sim}{x} - \underset{\sim}{\zeta}) \cdot \underset{\sim}{\phi}] + \nabla\phi_o\} ds , \quad (43a)$$

where $\underset{\sim}{\phi} = (\phi_1, \phi_2, \phi_3)$ and ϕ_o are harmonic functions and $\underset{\sim}{z}$ a constant vector,

$$\nabla^2 \underset{\sim}{\phi} = 0, \quad \nabla^2 \phi_o = 0, \quad \underset{\sim}{z} = (c_1, c_2, 0) \quad (43b)$$

Then the flow velocity generated by the same body shape _____ment in the presence of a wall coinciding with the $x_3 = 0$ plane is _____

$$\underset{\sim}{u} = \int_{-s_o}^{s_o} \{z\phi(\underset{\sim}{x};s,t) - \nabla[(\underset{\sim}{x} - \underset{\sim}{\zeta}) \cdot \underset{\sim}{\psi}] + \nabla\psi_o\} ds \quad (x_3 \geqslant 0), \quad (44)$$

where

$$\psi_o = \phi_o(\underset{\sim}{x}) - \hat{\phi}_o(\underset{\sim}{x}), \quad \hat{\phi}_o[x_1, x_2, x_3] = \phi_o[x_1, x_2, -x_3],$$

$$\underset{\sim}{\psi} = \underset{\sim}{\phi}(\underset{\sim}{x}) - \hat{\underset{\sim}{\phi}}(\underset{\sim}{x}) + 2e_3\{\frac{\partial}{\partial x_3}(\hat{\phi}_o - (\underset{\sim}{x} - \underset{\sim}{\zeta}) \cdot \hat{\underset{\sim}{\phi}}) + \nabla \cdot (x_3\hat{\underset{\sim}{\phi}})\} ,$$

$$\hat{\phi}[x_1, x_2, x_3] = \phi[x_1, x_2, -x_3] .$$

In the integral representation (43) of the unbounded flow, it is easy to identify the different terms in the integrand of (43) with various flow singularities. The representation (44) is obtained by appropriate imaging so that $u = 0$ at the wall $x_3 = 0$, and $\underset{\sim}{u}$ behaves like $\underset{\sim}{u}_o$ near the body. By expanding the integrals in (44) for the near field and applying the boundary condition (32), we can convert the resulting integral equation into a form similar to (38), and it can therefore be solved by the same iteration scheme. Numerical results are being analyzed for a few typical cases.

INERTIAL EFFECTS

Inertial effects will arise to effect changes in sectional force coefficients when either of the Reynolds numbers defined in (1) becomes no longer small compared to unity. Such situations may occur in motions of large micro-organisms or in experiments with mechanical models whose corresponding Reynolds numbers cannot all be kept small in practice.

A clear explanation of how inertial effects can arise has been provided by Chwang & Wu (1976) for a prolate spheroid. Even when the translational motion is directed only along the minor axis, with velocity U say, the solution is found to depend nevertheless on two Reynolds numbers, $R_a = Ua/\nu$ and $R_b = Ub/\nu$, based on the major and minor semi-axes a and b, respectively. The solution based on an approximate singular-perturbation method is shown to agree with the formula of Oberbeck (1876) for the Stokes flow as long as both R_a and R_b are small compared to unity, but deviates from it as R_a becomes of order unity, and finally approaches the Oseen's solution for a two-dimensional cylinder as $R_a \to \infty$, R_b being kept small throughout. This gradual transition thus provides a clear physical picture and explanation for the manifestation of the 'Stokes paradox' known in viscous flow theory.

It is thus important to have such inertial effects accounted for in making theoretical predictions and in interpreting experimental results. Development of the general slender-body theory along this line is still in its early stage, but is noted to be underway.

Recent development in cilia propulsion theory has been based on the 'envelope model', the 'sublayer-model', and the 'traction-layer model'. The historical background and principal new results have been extensively discussed and reviewed by Blake & Sleigh (1974), Keller, Wu & Brennen (1975), Wu (1976), Brennen & Winet (1977), so I shall not repeat here what is already available in the literature. However, I would like to apply again the 'traction-layer model' to make performance predictions on the basis of optimization calculation.

The traction-layer model is based on the concept that the discrete forces of a system of cilia can be represented by an 'equivalent' continuum distribution of an unsteady body force within the volume of the ciliary layer, provided the cilia distribution is sufficiently dense. Conversion from the discrete to the continuum force is based on resistive theory which relates the original sectional force of a cilium to its velocity relative to the flow produced in its neighborhood by the entire ciliary system.

Using this procedure the body force within a plane ciliary layer can be expressed as

$$f(x,y,t) = \sum_{n=0}^{N} f_n(y)e^{in(kx-\omega t)} \qquad (0 < y < l), \qquad (45)$$

where $N \ll \infty$, $\lambda = 2\pi/k$ is the metachronal wavelength, ω is the radian frequency, and f vanishes at the cell surface ($y = 0$) and also outside the cilia layer ($y \geqslant l$), l being the cilia length. The distribution functions $f_n(y)$ can be determined by carrying out the conversion from the discrete to continuum force. Since $f_n(y)$ are the Fourier coefficients of the continuum force at fixed y, the above expression for f holds valid for the general case of ciliary movements of finite amplitude.

The leading term of the expansion, $f_o(y)$, denotes the mean force distribution; it plays the essential role of providing the mean velocity field, $u_o(y)$, which satisfies the equation

$$\frac{\partial^2 u_o}{\partial y^2} = -\frac{1}{\mu} f_o(y).$$

In fact, the mean propulsion speed of the cilia layer is given by the value of u_o for $y > l$. The two functions f_o and u_o also determine the mean rate of working by f_o on the fluid in maintaining the mean velocity field, which is

$$E_o = \int_o^l f_o(y)u_o(y)\,dy. \qquad (46)$$

On the other hand, the rate of working by the cilia in producing f_o is

$$P_o = \int_o^l f_o(y)u_c(y)\,dy,$$

where $u_c(y)$ is the x-component of the mean velocity of cilia. Based on resistive-force theory, the ciliary force is proportional to the flow velocity relative to the ciliary segment, i.e. $f_o(y) = \mu C(u_c - u_o)$, C being a force coefficient. It therefore follows that the problem of extremizing E_o for

fixed P_o is equivalent to minimizing E_o for fixed mean square of f_o, or fixed

$$D_o = \int_o^l f_o^2(y)\,dy. \qquad (48)$$

Now the first variation of $E_o - \lambda D_o$, λ being an undetermined multiplier, gives

$$\delta(E_o - \lambda D_o) = l\int_o^l \{(u_o - 2\lambda f_o)\,\delta f_o(\eta) + f_o(\eta)\,\delta u_o(\eta)\}\,d\eta = 0,$$

where $\eta = y/l$. Substituting (46), or $\delta f_o = -\mu l^{-2}d^2(\delta u_o)/d\eta^2$, in the above integral and integrating by parts, we obtain for the first variation
$\delta(E_o - \lambda D_o) = 0$ the Euler equation

$$\frac{d^2 f_o}{d\eta^2} = -\frac{l^2}{\lambda\mu} f_o \qquad (0 \leqslant \eta \leqslant 1), \qquad (49)$$

$$\delta u_o = 0 \text{ and } \delta(du_o/d\eta) = 0 \qquad (\text{at } \eta = 0,1). \qquad (50)$$

The solution of (49) satisfying conditions $f_o(0) = f_o(1) = 0$ is the eigensolution

$$f_o(\eta) = \mu A \sin k_n\eta, \qquad k_n = (l^2/\mu\lambda_n)^{1/2} = n\pi, \qquad (51)$$

and the relevant solution corresponds to $n = 1$, $k_1 = \pi$. The resulting velocity, given by integrating (46) jointly with (51) under condition $u_o(0) = 0$ and $u'_o(\eta = 1) = 0$, is

$$u_o(\eta) = A(l/\pi)^2\,(\pi\eta + \sin\pi\eta) \qquad (0 < \eta < 1),$$

and $u_o(\eta) = \text{const.} = u_o(1)$ for $\eta > 1$. If $\tilde{D}_o = D_o/\mu^2 l = 1$ by normalization, then $A = \sqrt{2}$, and the corresponding $\tilde{E}_o = E_o/\mu l^3 = \sum (A/\pi)^2 = 3/\pi^2 = 0.304$.

The ratio $\tilde{E}_o/\tilde{D}_o = \mu E_o/D_o l^2 = 0.304$ gives the minimum energy imparted to fluid for fixed mean square force; this value is smaller than the four-term expansion of the optimum solution obtained previously by Wu (1976) (in the latter case $\tilde{E}_o/\tilde{D}_o = 0.364$, corresponding to about 20% more of the minimum specific work done). The mean force and mean velocity profile,

$$f_o/f_o^* = 2^{\frac{1}{2}}\sin\pi\eta, \qquad u_o/u_o^* = 2^{\frac{1}{2}}\pi^{-2}(\pi\eta + \sin\pi\eta), \qquad (53)$$

are shown in Fig. 9. (Here, in physical dimensions, $f_o^* = \mu\omega/kl^2$, and $u_o^* = \omega/k$ is the metachronal wave velocity.) The slope of $u_o(y)$ at $y = 0$, obtained by integrating (46) across the cilia layer, is related to the force integral by

$$\mu\frac{du_o(0)}{dy} = \int_o^l f_o(y)\,dy, \qquad (54)$$

which asserts that the viscous skin friction at cell surface is counterbalanced by the fluid force acting on the cilia over the same area of cell surface. The higher-order forcing functions $f_n(y)$ in the expansion (45) can also be optimized in a similar manner, but we shall not go into this here in
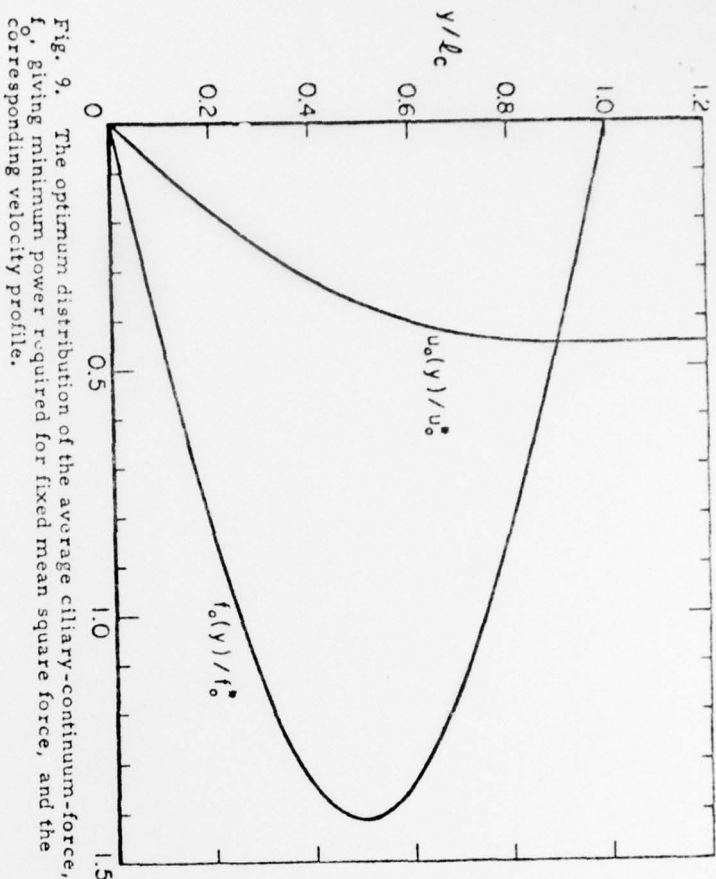
Fig. 9. The optimum distribution of the average ciliary-continuum-force, f_0, giving minimum power required for fixed mean square force, and the corresponding velocity profile.

STATE OF SELF-PROPULSION

We have just seen how the ciliary force can be optimally distributed when the curvature of the cell surface is zero. To extend this investigation to bodies of three-dimensional shapes, Keller & Wu (1977) have proposed a simple hydrodynamic model to determine the self-propulsion of ciliated micro-organisms and to examine the effect of body shape upon the velocity of propulsion. This model is a further generalization of the envelope model adopted by Blake (1971) and Brennen (1974) for considering the propulsion of spherically shaped micro-organisms (originally based on the assumption that the fluid adheres to a material envelope of the cilia ensemble), and is closely analogous to the control-surface model of Blake (1973). In the present control-surface model we consider the class of cilia envelopes of a prolate spheroidal shape, and assume that the mean flow velocity may have at the cilia envelope both a normal and a tangential component,

$$u_s = V_s \sin \theta , \qquad u_n = -V_n \cos \theta , \qquad (55)$$

where V_s and V_n are two constants and θ is the angle between the direction of propulsion and the unit outward normal $\hat{n}$ to the spheroidal control surface (see Fig. 10). The above simple relations represent the leading term of a more general variation in u_s and u_n along the cilia envelope; such aspects of flow behavior (as to have a normal flow velocity moving across the cilia envelope) have been supported by the observation of Cheung & Winet (1975).
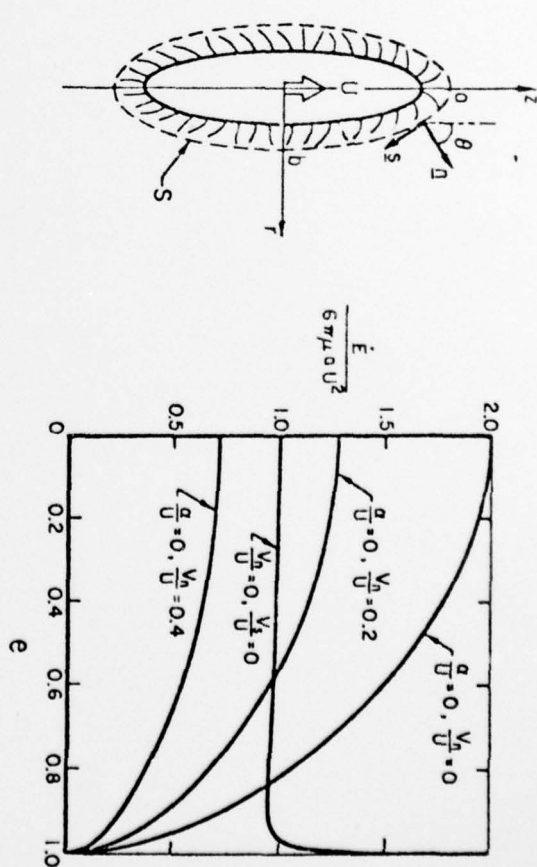

Fig. 10. The rate of energy cost for a prolate spheroid of constant volume and different eccentricity e. On the left the geometry of the control-surface model is shown with the cell body, the cilia layer and the control surface S.

The Stokes flow satisfying boundary condition (55) can be constructed by an axial distribution of Stokeslet and mass-doublet. The resulting energy expenditure, $\dot{E}$, is shown in Fig. 10 for spheroids of varying eccentricity e, the results being given with respect to the reference value of $6\pi\mu U^2 a$, where a and $b = a(1 - e^2)^{1/2}$ are the major and minor semi-axes, respectively. It is of significance to notice the following effect of body shape on energy expenditure. For the spherical shape (e = 0), the rate of working in moving a rigid sphere, of radius a, at velocity U is at the cost of an extraneous force F so that E = FU = $6\pi\mu U^2 a$. In comparison, a ciliated sphere with zero normal component of flow velocity ($V_n = 0$) and with the tangential component (V_s) so adjusted as to have zero force ($V_n = 0$) must spend energy $\dot{E} = 12\pi\mu U^2 a$ in maintaining the flow, which is then irrotational. Although the energy expenditure in the latter case is twice that for the rigid sphere, it does make a drastic distinction that the sphere with the slip-flow is capable of propelling itself! When the spheroid becomes slender, the energy required for propelling a spheroid with a slip flow actually turns out to be less than that for translating a no-slip spheroid of the same eccentricity e for e > 0.82. With the additional freedom of suction and blowing ($V_n \neq 0$) the energy cost can be further reduced (see, e.g. the curve with $V_n/U = 0.2$ in Fig. 10).

Streamlines of the resulting velocity field in the lab-frame are shown in Fig. 11 for the two basically different cases, one with slip-flow and the other satisfying the no-slip condition. In Fig. 12 two time exposures of two Paramecia, one self-propelling whereas the other being immobilized and

sedimenting under gravity. The observed streamlines in the case of free swimming evidently resemble those due to a doublet distribution, while the streamlines in the second case of sedimenting flow resemble another set due to a Stokeslet distribution. The analogy is of course not perfect, some minor discrepancy being primarily due to the presence of coverslip and side seals of the microscope slide.
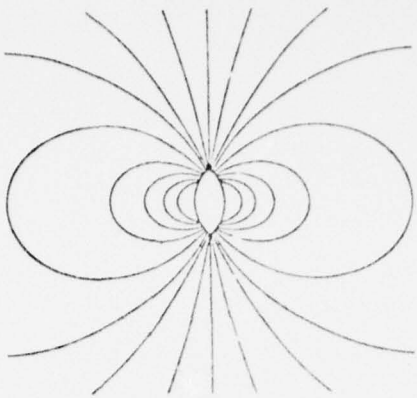
With this comparison, I hope the contrast is so sharp that it will help make an impression on the point I wish to make, namely: while there will always be stimulating problems along the frontier where the scheme of life is carrying on, one must be careful in scientific experimentation so as not to lose the basic element of life in its true manifestation.

Fig. 11. The streamlines (in the laboratory frame) of a self-propelling prolate spheroid of eccentricity 0.9 (upper) and of an externally-driven spheroid of the same shape (lower figure, with $V_s = V_n = 0$).
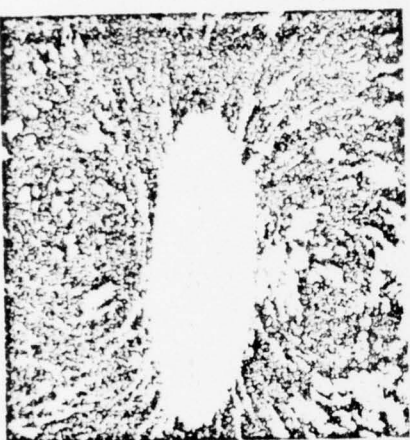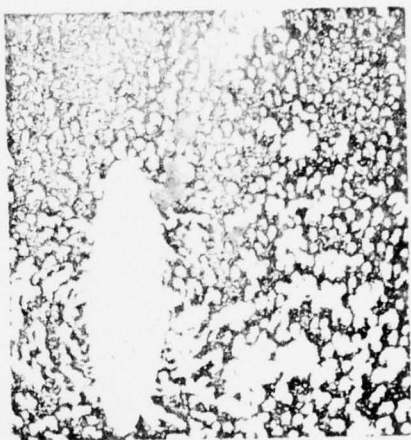
Fig. 12. Streak photographs of a freely swimming specimen of Paramecium caudatum (upper) and of a dead one sedimenting (towards right) under gravity (lower figure).

References

1 Aderogba, K., "On Stokeslets in Two-fluid Space," Journal of Engineering Mathematics, Vol. 10, 1976, pp. 143-151.

2 Batchelor, G. K., "Stress System in a Suspension of Force-free Particles," Journal of Fluid Mechanics, Vol. 41, 1970a, pp. 545-570.

3 Batchelor, G. K., "Slender Body Theory for Particles of Arbitrary Cross-section in Stokes Flow," Journal of Fluid Mechanics, Vol. 44, 1970b, pp. 419-440.

4 Blake, J. R., "A Spherical Envelope Approach to Ciliary Propulsion," Journal of Fluid Mechanics, Vol. 46, 1971a, pp. 199-208.

5 Blake, J. R., "Infinite Models for Ciliary Propulsion," Journal of Fluid Mechanics, Vol. 49, 1971b, pp. 209-222.

6 Blake, J. R., "A Note on the Image System for a Stokeslet in a No-Slip Boundary," Proceedings of the Cambridge Philosophical Society, Vol. 70, 1971c, pp. 303-310.

7 Blake, J.R., "A Model for the Micro-Structure in Ciliated Organisms," Journal of Fluid Mechanics, Vol. 55, 1972, pp. 1-23.

8 Blake, J.R. "A Finite Model for Ciliated Microorganisms," Journal of Biomechanics, Vol. 6, 1973, pp. 133-140.

9 Blake, J. R., "Hydrodynamic Calculations on the Movements of Cilia and Flagella. Part I. Paramecium," Journal of Theoretical Biology, Vol. 45, 1974a, pp. 183-203.

10 Blake, J. R., "Singularities of Viscous Flow. Part II. Applications to Slender Body Theory," Journal of Engineering Mathematics, Vol. 8, 1974b, pp. 113-124.

11 Blake, J. R., Chwang, A. T., "Fundamental Singularities of Viscous Flow. Part I. The Image Systems in the Vicinity of a Stationary No-Slip Boundary," Journal of Engineering Mathematics, Vol. 8, 1974, pp. 23-29.

12 Blake, J. R., Sleigh, M. A., "Mechanics of Ciliary Locomotion," Biological Reviews, Vol. 49, 1974, pp. 85-125.

13 Brennen, C., "An Oscillating-Boundary-Layer Theory for Ciliary Propulsion," Journal of Fluid Mechanics, Vol. 65, 1974, pp. 799-824.

14 Brennen, C., Winet, H., "Fluid Mechanics of Propulsion by Cilia and Flagella," Annual Review of Fluid Mechanics, Vol. 9, 1977, pp. 339-397.

15 Brenner, H., "Effect of Finite Boundaries on the Stokes Resistance of an Arbitrary Particle," Journal of Fluid Mechanics, Vol. 12, 1962, pp. 35-48.

16 Burgers, J.M., "On the Motion of Small Particles of Elongated Form Suspended in a Viscous Fluid," 2nd Rept. Visc. Plasticity Kon. Ned. Akad. Wet. Verhand., Vol. 16, 1938, pp. 113-184.

17 Cheung, A.T.W., Winet, H., "Flow Velocity Profile Over a Ciliated Surface. Eds. T. Y. Wu, C.J. Brokaw, C. Brennen, Swimming and Flying in Nature, Vol. 1, Plenum Press, New York, 1975, pp. 223-234.

18. Chwang, A. T., "Hydromechanics of Low-Reynolds-Number Flow. Part 3. Motion of a Spheroidal Particle in Quadratic Flows," Journal of Fluid Mechanics, Vol. 72, 1975, pp. 17-34.

19. Chwang, A., Winet, H., Wu, T. Y., "A Theoretical Mechanism for Spirochetal Locomotion," Journal of Mechano-Chemical and Cell Motility, Vol. 3, 1974, pp. 69-76.

20. Chwang, A. T., Wu, T. Y., "Proceedings of the Royal Society of London Series B, Microorganisms," Journal of Fluid Mechanics, Vol. 178, 1971, pp. 327-346.

21. Chwang, A. T., Wu, T. Y., "Hydromechanics of Low-Reynolds-Number Flow. Part 1. Rotation of Axisymmetric Prolate Bodies," Journal of Fluid Mechanics, Vol. 63, 1974, pp. 607-622.

22. Chwang, A. T., Wu, T. Y., "Hydromechanics of Low-Reynolds-Number Flow. Part 2. Singularity Method for Stokes Flows," Journal of Fluid Mechanics, Vol. 67, 1975a, pp. 787-815.

23. Chwang, A. T., Wu, T. Y., "Hydrodynamics of Flagellar Movements," Swimming and Flying in Nature, Eds. T. Y. Wu, C. J. Brokaw, C. Brennen, Vol. 1, 1975b, Plenum Press, New York, pp. 13-30.

24. Chwang, A. T., Wu, T. Y., "Hydromechanics of Low-Reynolds-Number Flow. Part 4. Translation of Spheroids," Journal of Fluid Mechanics, Vol. 75, 1976, pp. 677-689.

25. Cox, R. G., "The Motion of Long Slender Bodies in a Viscous Fluid. Part 1. General Theory," Journal of Fluid Mechanics, Vol. 44, 1970, pp. 791-810.

26. DeMestre, N. J., "Low-Reynolds Number Fall of Slender Cylinders Near Boundaries," Journal of Fluid Mechanics, Vol. 38, 1973, pp. 641-656.

27. DeMestre, N.J., Russel, W. B., "Low-Reynolds Number Translation of a Slender Cylinder Near a Plane Wall," Journal of Engineering Mathematics, Vol. 9, 1975, pp. 81-91.

28. Gray, J., 162 pp. "Ciliary Movement," Cambridge University Press, London, 1928.

29. Gray, J., "Animal Locomotion.", Norton, London, 1968, 479 pp.

30. Gray, J., Hancock, G.J., "The Propulsion of Sea-Urchin Spermatozoa," Journal of Experimental Biology, Vol. 32, 1955, pp. 802-814.

31. Hancock, G.J., "The Self-Propulsion of Microscopic Organisms Through Liquids," Proceedings of the Royal Society of London, Series A, Vol. 217, 1953, pp. 96-121.

32. Jahn, T. L., Votta, J.J., "Locomotion of Protozoa," Annual Review of Fluid Mechanics, Vol. 4, 1972, pp. 93-116.

33. Johnson, R.E., "Hydromechanics of Slender Bodies with Finite Curvature in Stokes Flow," Graduate Research Report, California Institute of Technology, 1976.

34. Katz, D. F., "On the Propulsion of Micro-organisms Near Solid Boundaries," Journal of Fluid Mechanics, Vol. 64, 1974, pp. 33-49.

35. Katz, D.F., Blake, J.R., "Flagellar Motions Near Walls," Eds. T. Y. Wu, C.J. Brokaw, C. Brennen, Swimming and Flying in Nature, Vol. 1, 1975, Plenum Press, New York, pp. 173-184.

36. Katz, D.F., Blake, J.R., Paveri-Fontana, S. L., "On the Movement of Slender Bodies Near Plane Boundaries at Low-Reynolds Number," Journal of Fluid Mechanics, Vol. 72, 1975, pp. 529-540.

37. Keller, J.B., Rubinow, S.I., "Slender-body Theory for Slow Viscous Flow," Journal of Fluid Mechanics, Vol. 75, 1976, pp. 705-714.

38. Keller, S. R., Wu, T. Y., "A Porous Prolate Spheroidal Model for Ciliated Microorganisms," Journal of Fluid Mechanics, 1977, (in press).

39. Keller, S. R., Wu, T. Y., Brennen, C., "A Traction Layer Model for Ciliary Propulsion," Swimming and Flying in Nature, Eds. T. Y. Wu, C.J. Brokaw, C. Brennen, Vol. 1, 1975, Plenum Press, New York.

40. Lighthill, M.J., "Hydromechanics of Aquatic Animal Propulsion," Annual Review of Fluid Mechanics, Vol. 1, 1969, pp. 413-445.

41. Lighthill, M.J., "Mathematical Biofluiddynamics," Society for Industrial and Applied Mathematics, 1975a, Philadelphia, 281 pp.

42. Lighthill, M.J., "Flagellar Hydrodynamics," The John vonNeuman Lecture, Society for Industrial and Applied Mathematics Reviews, 1975b.

43. Lorentz, H.A., "A General Theory Concerning the Motion of a Viscous Fluid and a Few Consequences Derived from it," Abhandlungen Theoretical Physics, Vol. 1, 1907, pp. 1-23.

44. Oberbeck, A., "Ueber Stationäre Flüssigkeitsbewegungen mit Berücksichtigung der inneren Reibung," Journal für die Reine und Angewandte Mathematik (Berlin), Vol. 81, 1876, pp. 62-80.

45. Oseen, C. W., "Hydrodynamik," Akademiya, Verlagsgesellschaft, 1927, Leipzig.

46. Sleigh, M.A., "Cilia and Flagella," Academic Press, 1974, New York, 500 pp.

47. Taylor, G.I., "Analysis of the Swimming of Microscopic Organisms," Proceedings of the Royal Society of London, Series A., Vol. 209, 1951, pp. 447-461.

48. Taylor, G.I., "The Action of Waving Cylindrical Tails in Propelling Microscopic Organisms," Proceedings of the Royal Society of London, Series A, Vol. 211, 1952a, pp. 225-239.

49. Taylor, G.I., "Analysis of Long and Narrow Animals," Proceedings of the Royal Society of London, Series A, Vol. 214, 1952b, pp. 158-183.

50. Tillett, J.P.K., "Axial and Transverse Stokes Flow Past Slender Axisymmetric Bodies," Journal of Fluid Mechanics, Vol. 44, 1970, pp. 401-417.

51. Tuck, E.O., "Some Methods for Flows Past Slender Slender Bodies," Journal of Fluid Mechanics, Vol. 18, 1964, pp. 619-635.

52. Winet, H., "Wall Drag on Free-moving Ciliated Microorganisms," Journal of Experimental Biology, Vol. 59, 1973, pp. 753-766.

53. Wu, T. Y., "Introduction to the Scaling of Aquatic Animal Locomotion," Scale Effects of Animal Locomotion, Eds. by J. Pedley, Academic Press, London, 1976, pp. 203-232.

54. Wu, T. Y., Brokaw, C.J., Brennen, C. (Eds.), Swimming and Flying in Nature, 2 Vols, Plenum Press, New York, 1975, 1005 pp.

55. Wu, T. Y., Johnson, R.E., "Hydromechanics of low-Reynolds-number flow. Part 5. Motion of a Slender Torus," Report ES 76-1, 1976, California Institute of Technology (to appear in publication).